CALCULATION of BURN-UP EFFECT on CONTROL ROD WORTH in VVER-1000 REACTOR

M. Kazem Dehdashti[a]

[a] Department of Nuclear Engineering, School of Mechanical Engineering, Shiraz University, Shiraz 71348-51154, Iran

Abstract

Knowledge of the control rod worth to absorb excess reactivity in a nuclear reactor core, is very important from many points of view. These include the analysis and the assessment of the shutdown margin of new core configurations as well as several operational needs, such as calibration of the control rods, in case that reactivity insertion experiments are planned. The control rod worth can be assessed through the utilization of neutronic codes. Control rods worth calculation is used to specify safety margin of reactor. The main goal of present study is to design a computational tool to calculation some safety neutronic parameters of a VVER-1000 reactor core such as control rod worth by effect of fuel Burn-Up in reactor first cycle operation. For the deterministic approach the neutronics code system MCNPX is used. To achieve this goal, first, some reactor operation states with different power density distribution are obtained by positioning the control rods in different configurations. The control rod worth for each corresponding state are calculated using a reactor validated model developed in MCNPX 2.7 code. The results of this study indicates that the control rod worth can be determined through a MCNPX model.

Keywords: Control rod worth, Fuel Burn-up, Power peaking factor (PPF), MCNPX code, Reactivity

1. Introduction

An accurate prediction on the neutronic parameters of a nuclear reactor core is a major concept in its design for both economic and safety reasons. Development of economically beneficial and safe operation conditions requires more accurate, comprehensive and real-time analysis of the neutronic parameters (IAEA, 2005). In order to meet the various safety requirements imposed on the fuel pellets and fuel clad barriers such as the local power density (LPD) and the departure from nucleate boiling ratio (DNBR), which play an important role in the protection and monitoring systems, are not violated during the reactor's operation a real-time monitoring system is required (Wang et al., 2003). The changes in reactor core power distribution are usually monitored by detecting the neutron flux density via the protection system which uses in-core and ex-core neutron detectors signals. Early monitoring of the reactor power distribution and power peaking factor measurement are performed by the miniature fission chamber neutron detectors installed in the in-core instrument channels and the calculation of the power distribution is carried out with the help of a series of neutron flux data. However, utilizing the in-core neutron detectors to accurately compute the power distribution and the other real-time parameters is faced with some problems. Core size, high temperature, high pressure and some special materials proposes in the core are limitations of using in-core detectors in some cases (Bae et al., 2009). The purpose of creating an ex-core instrumentation system for advanced reactors, including VVER-1000 reactors, is to increase the safety and efficiency of nuclear power plant (NPP) operation, by increasing the response speed, reliability and accuracy of the operational monitoring system.

The main goal of this study is to predict the radial and axial RPDs and PPF in a VVER1000 reactor core using measured signals of the reactor coolant system, ex-core neutron detectors, power level, and control

rods position. By studying the complex relationship between the power distribution change, core neutron flux change and ex-core neutron detector response, we find out that artificial neural networks (ANNs) could properly fit the complex nonlinear function of these aspects.

ANNs allow modelling complex systems without requiring an explicit knowledge or formulation of the relationship that exist among the variables and constitute an alternative to structured models or empirical correlations (Hassoun, 1995). ANNs have been successfully applied to different applications in nuclear engineering from nuclear reactor dynamics simulation to the PPF estimation and the 3D power distribution prediction (Pirouzmand et al., 2011; Hadad and Pirouzmand, 2007; Tanabe and Yamamoto, 1993; Nae et al., 2004; Mary et al., 2006; Montes and Francois, 2009; Xia et al., 2013). This work proposes a method, based on the artificial neural network technique to predict the radial and axial RPDs and PPF accurately in real-time. To verify the validity of this method, a series of experimental data taken from the Bushehr nuclear power plant (BNPP) are used. All of these parameters are usually deduced from the core variables such as the signals from ex-core detectors, position of control rods, power level, coolant inlet temperature, and boric acid concentration.

2. VVER-1000 reactor core

VVER-1000 reactor core can be divided into similar 60^0 (degree) symmetry each one contain 28 segments (FAs). As long as the neutron flux of each segment is obtained, the axial RPD of the core can be calculated in certain conditions. When the reactor core operates at hot zero power, each segment can be viewed as a neutron source and the neutron leakage from each segment is almost constant and that is monitored by ex-core neutron detectors. The escaped neutrons can cross over the surrounding segments, the reflective layer, and the pressure vessel and finally reach to the ex-core detectors. Meanwhile, the count of the detector is the superposition of the neutrons leaked from each segment. Therefore, a correspondent relationship would exist between the measured data and the neutron flux density value of each segment. In addition, for neutron flux, there is a strong correlation between each segment, especially between adjacent ones. Also the change of the neutron flux in one segment interacts neighboring segments as well as remote segments. The ex-core neutron detector is extremely sensitive to the neutron flux change of the peripheral segment. Consequently, the change of the core neutron flux distribution can be deduced from the count rate of the ex-core neutron detectors (Xia et al., 2013).

The ex-core neutron detectors of the VVER-1000 reactor together with the corresponding electronic systems can monitor the core's neutron leakage under power operation within the range of (10^{-9} to 120) % rated power. In addition, the ex-core measurement system provides some critical core parameters such as reactor period over the range of (10 to 500) seconds, reactivity, monitoring of neutron flux during start-up of reactor and reactor core loading (refuelling). Fig.1 shows the ex-core neutron detectors arrangement around the core in instrumentation and control (I&C) channels. There are provided 15 neutron detector channels in the biological shield with different measuring level. Measuring level is divided into three groups; consist of start-up, operation and source ranges. The channels 1, 6, and 12 measure the neutron leakage during the start-up and operation ranges, the channels 3, 7, and 11 are used during source range, and the channels 4, 9, 15, 2, and 13 are responsible of measurement during the source range. The detectors are located in two different vertical levels. The main task of the ex-core nuclear measurement system is to alarm timely during steady power operation and active the shutdown system when it is needed, by monitoring the neutron flux. This research addresses the RPD and PPF

predictions from the ex-core measurement system in 1/6 core symmetry. Here, the signal of one neutron detector is used for the neural networks training, validation and testing (AEOI, 2007).

3. MCNPX Model

A Monte Carlo method does not solve an explicit equation like a deterministic code; it rather calculates the solutions by simulating individual particles and recording some aspects (tallies) of their average behavior. Monte Carlo codes make use of a continuous energy scale to represent the variation of the cross section data that are widely used because of their capability in modeling of complex geometries (Dunn and Shultis, 2011). MCNPX 2.7 which is a Monte Carlo based computer code and has some features such

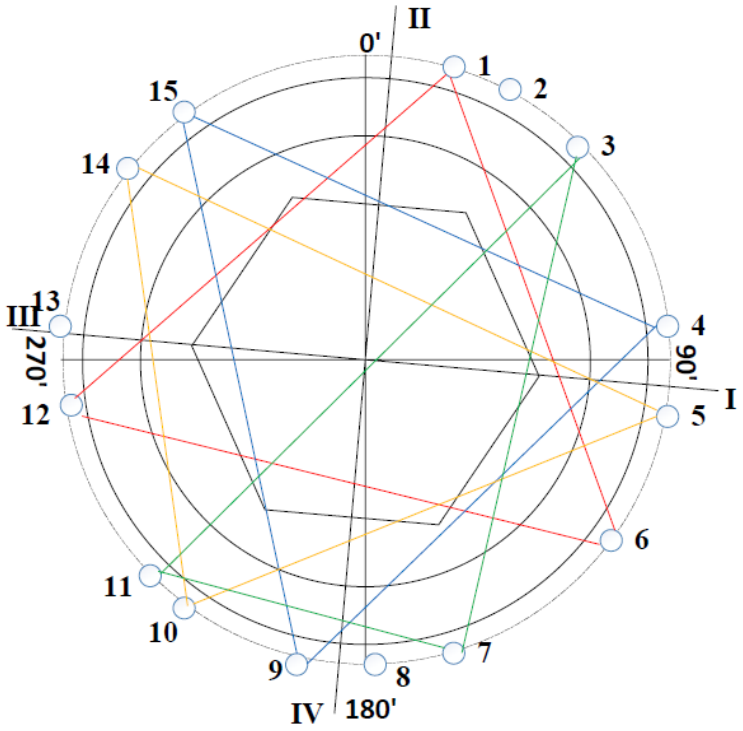

Fig. 1. Diagram of detection unit arrangement in I&C channels (AEOI, 2007)

As being general-purpose, continuous-energy, generalized-geometry, burnup calculation, and various particle transport calculation is used in this research for RPD and PPF calculations (Pelowitz, 2008).

In this study, a VVER-1000 reactor core model is designed and developed by MCNPX 2.7 code. The model contains all physical core components in real reactor operation conditions. Different tallies are considered in this model to calculate the axial and radial relative power distributions. All fuel rods (material and clad), water channels, guide channels and control rods are divided to ten axial nodes to consider the effect of coolant temperature and density distributions on the core axial relative power calculations. Axial temperature distribution for each core state is calculated using a model of VVER-1000 reactor based on Unit 1 of BNPP developed in RELAP5/MOD3.2 code consists of 4-loop primary and secondary systems with all their relevant sub-systems (Pirouzmand et al., 2014). The RPD is affected by major factors such

as: the time of operation, the coolant inlet temperature, the position of control rods groups, the power level, and the boric acid concentration. Fig. 2 shows BNPP VVER-1000 core configuration including different fuel assemblies (FAs) with corresponding enrichment value at the first fuel cycle. Also, Table 1 presents the characteristics of different FA types are used at the first fuel cycle (AEOI, 2007).

The MCNPX model is validated against BNPP FSAR and neutron album data during the first fuel cycle. The calculation is carried out in the first fuel cycle for 0.00 to 293.82 days of operation with variation in the control rods position, the boric acid concentration, the power level, and the coolant inlet temperature. Also, many actual steady state and transient reactor operation states with different effective factors are applied to calculate axial and radial RPDs for each FA in ten axial nodes.

Table 2 presents some part of the MCNPX model results that are compared with BNPP neutron album (BNPPNA) data. In this table T_{eff}, T_{in}, H10, P, C_{bc}, K_q, K_v, N_k, and N_z are the time of reactor operation, core inlet temperature, position of control rods group 10 (percent of withdrawn length), power level, boric acid concentration, radial and axial PPFs, FA number, and core axial level, respectively.

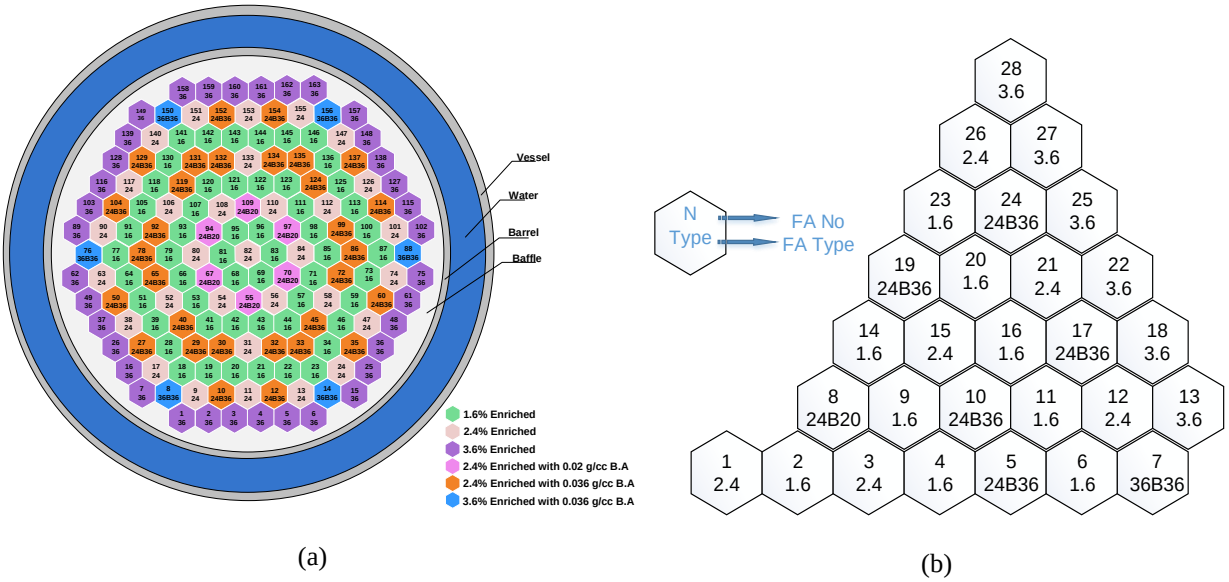

(a) (b)

Fig .2. VVER-1000 core configuration including different FAs in the first fuel cycle (a) whole core and (b) 1/6 core symmetry (AEOI, 2007).

Table 1. Description of FA types used in the first fuel cycle (AEOI, 2007).

FA type	Average Enrichment (U_{235} , % weight)	Number of fuel rods type 1 (% enrichment)	Number of fuel rods type 2 (% enrichment)	Number of burnable absorber rods	Boron concentration [g/cm^3]
1.6	1.6	1.6(311)	-	-	-
2.4	2.4	2.4(311)	-	-	-
3.6	3.6	3.7(245)	3.3(66)	-	-
24B20	2.4	2.4(311)	-	18	0.020
24B36	2.4	2.4(311)	-	18	0.036
36B20	3.6	3.7(245)	3.3(66)	18	0.020

Table 2. The calculated MCNPX model results compared with BNPPNA data.

					BNPPNA (AEOI, 2004)		**MCNPX Model**	
T_{eff} [day]	T_{in} [ºC]	H10 [%]	P [MW]	C_{bc} [g/kg]	K_q [relative, N_k]	K_v [relative, N_k,N_z]	K_q [relative ,N_k]	K_v [relative ,N_k,N_z]
0	280.5	60	150	6.83	1.42 25	2.07 25 5	1.42 25	2.07 25 5
1	282.8	60	750	6.04	1.34 21	1.90 21 4	1.34 21	1.90 21 4
5	284.4	70	1200	5.6	1.29 21	1.78 21 5	1.29 21	1.78 21 5
10	285.5	80	1500	5.36	1.26 21	1.71 21 5	1.26 21	1.71 21 5
15	285.5	80	1500	5.3	1.26 21	1.69 21 5	1.25 21	1.67 21 5
20	288.3	80	2250	4.95	1.22 21	1.66 21 4	1.22 21	1.66 21 4
40	288.3	80	2250	4.74	1.22 1	1.60 1 5	1.22 1	1.60 1 5
60	288.3	80	2250	4.16	1.22 1	1.52 3 5	1.22 1	1.52 3 5
70	288.3	80	2700	3.93	1.24 1	1.52 3 4	1.23 1	1.50 3 4
80	291	90	3000	3.93	1.24 1	1.45 3 4	1.24 1	1.44 3 4
100	291	90	3000	3.58	1.22 3	1.39 3 3	1.21 3	1.39 3 3
120	291	90	3000	2.23	1.21 3	1.37 3 3	1.21 3	1.35 3 3
160	291	90	3000	2.51	1.19 3	1.32 3 3	1.18 3	1.32 3 3
200	291	90	3000	1.76	1.17 3	1.31 3 2	1.17 3	1.31 3 2
240	291	90	3000	1.01	1.15 3	1.31 15 2	1.15 3	1.31 15 2
260	291	90	3000	0.63	1.15 3	1.31 15 2	1.14 3	1.31 15 2
293	291	90	3000	0	1.14 3	1.30 15 2	1.14 3	1.30 15 2
293 .82	291	90	3000	0	1.14 3	1.30 15 2	1.14 3	1.29 15 2

The calculated average error of MCNPX model results for all operation states given in Table 2 are shown in Fig. 3. The maximum error is less than 1.5% and 1% for axial and radial data (respectively) which is accurate enough to be used in RPD monitoring.

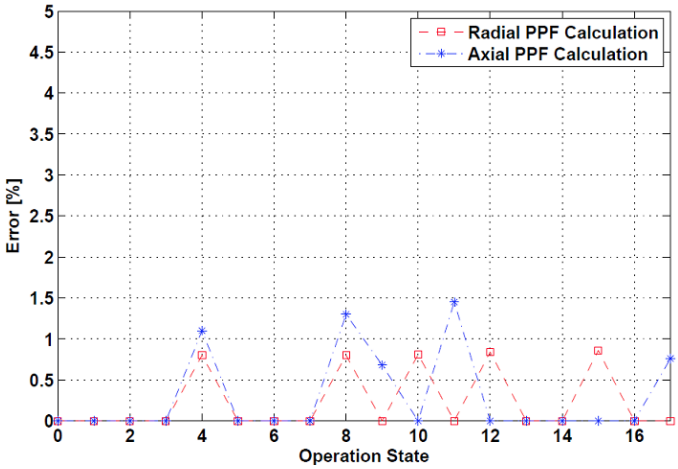

Fig. 3. Calculated average error of MCNPX model results for all operation states given in Table 2.

Table 3. One of reactor operation state investigated for MCNPX model validation

Reactor core parameter	Si_{ex} [A]	H8 [%]	H9 [%]	H10 [%]	C_{bc} [g/kg]	T_{in} [ºC]	P [MW]	T_{eff} [day]

Value	8.23E-05	100	100	70	5.6	284.4	1200	5

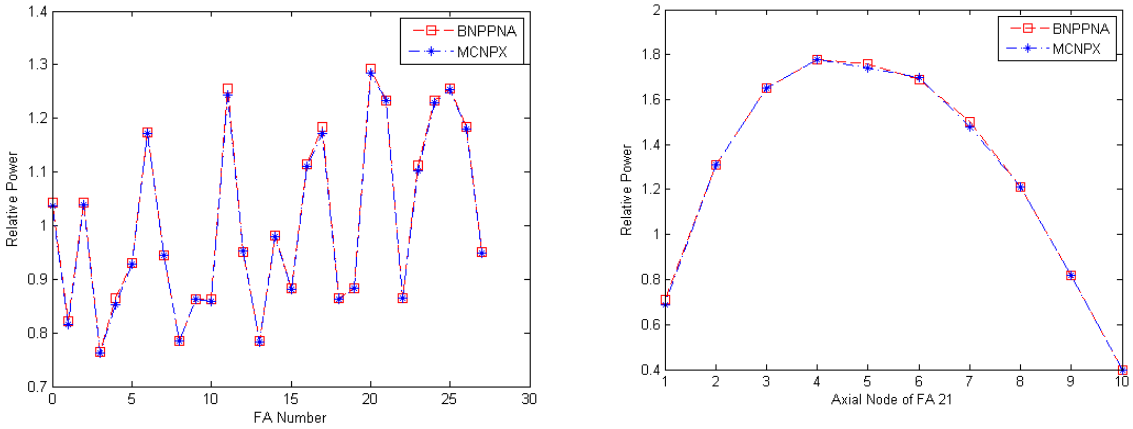

(a) (b)

Fig. 4. Comparison of the MCNPX model results with BNPP neutron album data (a) radial and (b) axial relative power for the operation state given in Table 3.

Also, Fig. 4 illustrates the radial and axial RPDs for an operation state with reactor core parameters given in Table 3 for further comparison. As shown there is a very good comparison between the MCNPX model results and the BNPPNA data. In this table H8, H9 and Si_{ex} are the position of control rods group 8 and 9 and the signal of ex-core neutron detector, respectively.

7. Conclusion

This paper introduced a new tool for RPD and PPF predictions in a VVER reactor core based on an ANN framework and a series of experimental reactor operation data that were used for network training, validation and testing to develop an accurate monitoring system which can be incorporated into the reactor protection system. The ANN technique was chosen to develop the monitoring system due to its ability in the complex and non-linear problems modelling in real-time. MLP networks with different number of hidden layers and various number of neurons in each layer were examined for this application. Based on the results, finally, an MLP network with two hidden layers was chosen.

In this research, 200 reactor operation states with different power density distributions were considered in 1/6 core symmetry for the ANN training, validation and testing. For each state RPD and PPF values were calculated using a verified MCNPX model of BNPP. The performance of proposed ANN was evaluated by MSE calculation and regression plot that show an average MSE less than 0.6 percent and an R value greater than 0.99. Also the error aggregation was observed to occur around the minimum error which is a criterion for a neural network with efficient performance (Fig. 6(b)).

Investigation of different core parameters used in training process showed that the RPD change is extremely sensitive to the position of control rods groups and signal of ex-core neutron detector. To express the importance of ex-core neutron detector signal's role in network's response, the ex-core signal

was omitted from all input data in network's training process. The MSE value and error aggregation plots revealed that the network's performance is getting worst (Fig. 8). This demonstrates the necessity of ex-core detector signals application for an accurate and reliable estimation of radial and axial RPDs and PPF using ANNs.

Finally, the ability of MLP network in real-time prediction of RPD and PPF was assessed for various practical core states which were not used in training, validation, and testing processes. The results illustrates the capability and high accuracy of the proposed MLP network in RPD and PPF predictions. As illustrated in Fig. 12 the maximum value of error is less than 3%.

In conclusion, the results of this study indicates that the RPD and PPF in a VVER-1000 reactor core can be determined accurately through an ANN having as input the position of control rods, core inlet temperature, power level, coolant inlet temperature, acid boric concentration, effective days of reactor operation, and signal of ex-core detectors.

References

Atomic Energy Organization of Iran (AEOI), (2007), BUSHEHR Nuclear Power Plant FSAR, Chapter 7: Instrumentation and control systems (I&C)", Book1.

Atomic Energy Organization of Iran (AEOI), (2004), Album of Neutron and physical Characteristics of The 1-st Loading of BNPP, Organization of Activities on BNPP-1Commissioning.

Bae, I.H., Gyun, M., Lee, Y.J and Park, G.C., (2009), Estimation of The Power Peking Factor in Nuclear Reactor Using Support Vector Machine, Nuclear Engineering and Technology, vol.41, pp.1181.

Beale, M.H., Hagan, M.T. and Demuth, H.B., (2014), Neural Network Toolbox User's Guide, the Math Works, Inc.

Briemeister, J.F., (2013), MCNPX "A General Monte Carlo N-Particle Transport Code, Version X.2.7, Los Alamos National Laboratory, La-13709.

Dunn, W.L. and Shultis, J.K., (2011), Exploring Monte Carlo Methods, 1st Edition, Elsevier science.

Hadad, K., Piroozmand, A., (2007), Application of cellular neural network (CNN) method to the nuclear reactor dynamics equations, Annals of Nuclear Energy, Vol.34, pp.406-416.

Hassoun, M., (2003), Fundamentals of Artificial Neural Networks, a Bradford Book.

International Atomic Energy Agency, (2005), Safety Standards Design of the Reactor Core for Nuclear Power Plants for protecting people and the environment, Design of the Reactor Core for Nuclear Power Plants

Mary, R., Souza, G.P. and Moreira, M.L., (2006), Neural Network Correlation for Power Peaking Factor Estimation, Annals of Nuclear Energy, vol.33, pp.594-608.

Montes, J.L. and Francois, J., (2009), Local Power Peaking Factor Estimation in Nuclear Fuel by Artificial Neural Networks, Annals of Nuclear Energy, Vol. 36, pp. 121-130.

Nae, M., Jung, D.W. and Shin, S.H., (2004), Estimation of the Nuclear Power Peaking Factor Using In-core Sensor Signals, Korean Nuclear Society, Vol. 36, pp. 420-429.

Pelowitz, D.B., (2008), MCNPX USER'S MANUAL, Version 2.6.0, LA-CP-07-1473.

Pirouzmand, A., Ghasemi, A. and Faghihi, F., (2014), Safety Analysis of LBLOCA with Station Blackout for the BUSHEHR's VVER-1000 Nuclear Power Plant, Nurer2014 conference, Antalya, Turkey.

Pirouzmand, A., Hadad, K., (2011), Cellular neural network to the spherical harmonics approximation of neutron transport equation in x–y geometry Part I: Modeling and verification for time-independent solution, Annals of Nuclear Energy, Vol.47, pp.225-233.

Tanabe, A. and Yamamoto, T., (1993), Development of Neural Network for Analysis of Local Power Distributions in Bare Fuel Bundles, Nuclear Science and Technology, Vol. 30, pp. 804-812.

Wang, Y., Zhengpei, F.L and Han, S., (2003), On-line Monitoring the In-Core Power Distribution by Using Ex-core Ion-Chambers, Nuclear Engineering and Design, Vol.225, pp.315-326.

Xia, J., Li, B. and Liu, J., (2013), Research on intelligent monitor for 3D Power Distribution of Reactor Core, Annals of Nuclear Energy, Vol.73, Pages 446–454.

++

1. Introduction

2. Control rod worth calculation

3. Power distribution for control rod insertion

4. Results

UP%C R8	UP%C R9	UP%C R10	TIME day	$\Delta\rho_{gr}$,% INTEGRAL BNPP	$\Delta\rho_{gr}$,% INTEGRAL MCNPX	$\Delta\rho_{CPS}$,% INDIVIDUAL BNPP	$\Delta\rho_{CPS}$,% INDIVIDUAL MCNPX	$\partial\rho/\partial H$ *10³%/cm BNPP	$\partial\rho/\partial H$ *10³%/cm MCNPX	$C_{bc\ g/Kg}$	$T_{in\ C'}$	$\%N_{power}$ MW
--	--	0	0	--	--	-0.164	-0.137	--	0.38	16	280	0
--	0	0	0	-0.798	-0.746	-0.635	-0.609	--	1.71	16	280	0
0	0	0	0	-2.110	-2.023	-1.312	-1.277	--	3.59	16	280	0
100	100	100	0	--	--	--	--	--	--	7.33	280	0
100	100	90	0	0.00	0.00	0.00	0.00	0.11	0.00	7.33	280	0
100	100	80	0	-0.02	-0.02	-0.02	-0.02	0.42	0.56	7.32	280	0
100	100	70	0	-0.05	-0.06	-0.03	-0.04	0.84	1.12	7.30	280	0
100	100	60	0	-0.09	-0.10	-0.04	-0.04	1.30	1.27	7.28	280	0
100	100	50	0	-0.15	-0.16	-0.06	-0.06	1.71	1.69	7.25	280	0
100	100	40	0	-0.22	-0.23	-0.07	-0.07	1.99	1.97	7.21	280	0
100	100	30	0	-0.29	-0.29	-0.07	-0.06	1.94	1.95	7.18	280	0
100	100	20	0	-0.34	-0.33	-0.05	-0.04	1.46	1.38	7.15	280	0
100	100	10	0	-0.37	-0.36	-0.03	-0.03	0.77	0.84	7.14	280	0
100	100	00	0	-0.38	-0.39	-0.01	0.0	0.25	0.00	7.13	280	0
100	100	100	5	--	--	--	--	--	--	5.65	284.4	40
100	100	90	5	-0.01	-0.01	-0.01	-0.01	0.40	0.42	5.65	284.4	40
100	100	80	5	-0.06	-0.05	-0.05	-0.04	1.16	1.14	5.63	284.4	40
100	100	70	5	-0.12	-0.11	-0.06	-0.06	1.79	1.79	5.60	284.4	40
100	100	60	5	-0.20	-0.19	-0.08	-0.08	2.21	2.25	5.56	284.4	40
100	100	50	5	-0.29	-0.27	-0.09	-0.08	2.51	2.38	5.51	284.4	40
100	100	40	5	-0.38	-0.36	-0.09	-0.09	2.72	2.68	5.47	284.4	40
100	100	30	5	-0.48	-0.46	-0.10	-0.10	2.76	2.81	5.42	284.4	40

100	100	20	5	-0.56	-0.54	-0.08	-0.08	2.44	2.38	5.37	284.4	40
100	100	10	5	-0.62	-0.58	-0.06	-0.04	1.62	1.46	5.35	284.4	40
100	100	00	5	-0.64	-0.61	-0.02	-0.03	0.65	0.84	5.33	284.4	40
100	100	100	50	--	--	--	--	--	--	4.65	288.3	75
100	100	90	50	-0.02	-0.01	-0.02	-0.01	0.56	0.53	4.64	288.3	75
100	100	80	50	-0.07	-0.06	-0.05	-0.05	1.55	1.52	4.61	288.3	75
100	100	70	50	-0.16	-0.15	-0.09	-0.09	2.30	2.53	4.57	288.3	75
100	100	60	50	-0.25	-0.25	-0.09	-0.10	2.70	2.81	4.52	288.3	75
100	100	50	50	-0.35	-0.35	-0.10	-0.10	2.92	3.09	4.47	288.3	75
100	100	40	50	-0.46	-0.47	-0.11	-0.12	3.07	3.38	4.42	288.3	75
100	100	30	50	-0.57	-0.58	-0.11	-0.11	3.12	3.09	4.36	288.3	75
100	100	20	50	-0.67	-0.67	-0.10	-0.09	2.94	2.80	4.31	288.3	75
100	100	10	50	-0.75	-0.75	-0.08	-0.08	2.19	2.25	4.27	288.3	75
100	100	00	50	-0.79	-0.79	-0.04	-0.04	0.98	1.12	4.25	288.3	75
100	100	100	70	--	--	--	--	--	--	4.20	289.9	90
100	100	90	70	-0.02	-0.02	-0.02	-0.02	0.70	0.67	4.19	289.9	90
100	100	80	70	-0.09	-0.10	-0.07	-0.08	1.86	2.16	4.16	289.9	90
100	100	70	70	-0.18	-0.19	-0.09	-0.09	2.60	2.56	4.11	289.9	90
100	100	60	70	-0.28	-0.29	-0.10	-0.10	2.88	2.81	4.06	289.9	90
100	100	50	70	-0.39	-0.41	-0.11	-0.12	2.96	3.29	4.00	289.9	90
100	100	40	70	-0.49	-0.53	-0.10	-0.12	3.01	3.26	3.95	289.9	90
100	100	30	70	-0.60	-0.64	-0.11	-0.11	3.04	3.09	3.90	289.9	90
100	100	20	70	-0.70	-0.73	-0.10	-0.09	2.94	2.80	3.84	289.9	90
100	100	10	70	-0.79	-0.82	-0.09	-0.09	2.33	2.39	3.80	289.9	90
100	100	00	70	-0.82	-0.85	-0.03	-0.03	1.11	1.01	3.78	289.9	90
100	100	100	100	--	--	--	--	--	--	5.75	291	0
100	100	90	100	-0.02	-0.02	-0.02	-0.02	0.68	0.56	5.74	291	0
100	100	80	100	-0.09	-0.09	-0.07	-0.07	1.81	1.86	5.71	291	0

100	100	70	100	-0.17	-0.16	-0.08	-0.07	2.35	2.20	5.67	291	0
100	100	60	100	-0.26	-0.26	-0.09	-0.10	2.39	2.70	5.62	291	0
100	100	50	100	-0.34	-0.35	-0.08	-0.09	2.31	2.42	5.58	291	0
100	100	40	100	-0.41	-0.42	-0.07	-0.07	2.23	2.20	5.54	291	0
100	100	30	100	-0.48	-0.47	-0.07	-0.05	2.04	1.76	5.51	291	0
100	100	20	100	-0.54	-0.53	-0.06	-0.06	1.53	1.57	5.48	291	0
100	100	10	100	-0.56	-0.55	-0.02	-0.02	0.82	0.74	5.47	291	0
100	100	00	100	-0.57	-0.56	-0.01	-0.01	0.27	0.25	5.46	291	0
100	100	100	100	--	--	--	--	--	--	3.60	291	100
100	100	90	100	-0.03	-0.03	-0.03	-0.03	0.87	0.84	3.58	291	100
100	100	80	100	-0.11	-0.10	-0.08	-0.07	2.18	2.20	3.54	291	100
100	100	70	100	-0.21	-0.19	-0.10	-0.09	2.84	2.80	3.49	291	100
100	100	60	100	-0.31	-0.29	-0.10	-0.10	2.95	2.93	3.44	291	100
100	100	50	100	-0.42	-0.40	-0.11	-0.11	2.90	2.98	3.38	291	100
100	100	40	100	-0.52	-0.50	-0.10	-0.10	2.87	2.81	3.33	291	100
100	100	30	100	-0.62	-0.59	-0.10	-0.09	2.90	2.80	3.28	291	100
100	100	20	100	-0.72	-0.68	-0.10	-0.09	2.89	2.83	3.22	291	100
100	100	10	100	-0.81	-0.76	-0.09	-0.08	2.46	2.38	3.18	291	100
100	100	00	100	-0.85	-0.80	-0.04	-0.04	1.25	1.27	3.16	291	100
100	100	100	200	--	--	--	--	--	--	4.17	291	0
100	100	90	200	-0.06	-0.06	-0.06	-0.06	1.77	1.79	4.14	291	0
100	100	80	200	-0.19	-0.19	-0.13	-0.13	3.56	3.66	4.08	291	0
100	100	70	200	-0.31	-0.29	-0.12	-0.10	3.55	3.55	4.01	291	0
100	100	60	200	-0.41	-0.38	-0.10	-0.09	2.79	2.80	3.96	291	0
100	100	50	200	-0.48	-0.45	-0.07	-0.07	2.10	2.20	3.93	291	0
100	100	40	200	-0.54	-0.50	-0.06	-0.05	1.58	1.52	3.90	291	0
100	100	30	200	-0.58	-0.54	-0.04	-0.04	1.12	1.12	3.88	291	0
100	100	20	200	-0.60	-0.56	-0.02	-0.02	0.71	0.74	3.87	291	0

100	100	10	200	-0.61	-0.57	-0.01	-0.01	0.36	0.34	3.86	291	0
100	100	00	200	-0.62	-0.58	-0.01	-0.01	0.13	0.18	3.86	291	0
100	100	100	200	--	--	--	--	--	--	1.79	291	100
100	100	90	200	-0.05	-0.05	-0.05	-0.05	1.43	1.52	1.76	291	100
100	100	80	200	-0.15	-0.13	-0.10	-0.08	2.95	2.84	1.71	291	100
100	100	70	200	-0.27	-0.24	-0.12	-0.11	3.24	3.21	1.65	291	100
100	100	60	200	-0.37	-0.34	-0.10	-0.10	2.94	2.97	1.59	291	100
100	100	50	200	-0.47	-0.45	-0.10	-0.11	2.66	2.70	1.54	291	100
100	100	40	200	-0.56	-0.56	-0.11	-0.11	2.51	2.62	1.50	291	100
100	100	30	200	-0.64	-0.64	-0.08	-0.08	2.47	2.44	1.45	291	100
100	100	20	200	-0.73	-0.73	-0.09	-0.09	2.54	2.53	1.41	291	100
100	100	10	200	-0.82	-0.79	-0.09	-0.06	2.40	2.20	1.36	291	100
100	100	00	200	-0.87	-0.84	-0.05	-0.05	1.40	1.46	1.34	291	100
100	100	100	293.82	--	--	--	--	--	--	2.62	291	0
100	100	90	293.82	-0.10	-0.08	-0.10	-0.08	2.77	2.68	2.57	291	0
100	100	80	293.82	-0.26	-0.24	-0.16	-0.16	4.73	4.70	2.49	291	0
100	100	70	293.82	-0.41	-0.39	-0.15	-0.15	4.11	4.17	2.42	291	0
100	100	60	293.82	-0.51	-0.49	-0.10	-0.10	2.82	2.81	2.37	291	0
100	100	50	293.82	-0.57	-0.55	-0.07	-0.06	1.78	1.79	2.34	291	0
100	100	40	293.82	-0.61	-0.59	-0.04	-0.04	1.04	1.12	2.32	291	0
100	100	30	293.82	-0.62	-0.62	-0.01	-0.03	0.55	0.56	2.32	291	0
100	100	20	293.82	-0.63	-0.63	-0.01	-0.01	0.28	0.24	2.31	291	0
100	100	10	293.82	-0.64	-0.64	-0.01	-0.01	0.14	0.18	2.31	291	0
100	100	00	293.82	-0.64	-0.64	0.0	0.0	0.05	0.00	2.31	291	0
100	100	100	293.82	0.07	0.07	--	--	--	--	0.00	291	100
100	100	90	293.82	0.00	0.00	-0.07	-0.07	1.88	1.86	0.00	291	100
100	100	80	293.82	-0.12	-0.05	-0.05	-0.05	3.46	1.76	0.00	291	100
100	100	70	293.82	-0.24	-0.17	-0.12	-0.12	3.44	3.38	0.00	291	100

100	100	60	293.82	-0.35	-0.28	-0.11	-0.11	2.98	2.98	0.00	291	100
100	100	50	293.82	-0.44	-0.38	-0.09	-0.10	2.64	2.70	0.00	291	100
100	100	40	293.82	-0.53	-0.46	-0.09	-0.09	2.42	2.42	0.00	291	100
100	100	30	293.82	-0.61	-0.54	-0.08	-0.08	2.28	2.25	0.00	291	100
100	100	20	293.82	-0.69	-0.62	-0.08	-0.08	2.26	2.25	0.00	291	100
100	100	10	293.82	-0.77	-0.69	-0.08	-0.07	2.17	2.19	0.00	291	100
100	100	00	293.82	-0.81	-0.73	-0.04	-0.04	1.34	1.38	0.00	291	100
100	100	00	0	--	--	--	--	--	--	7.13	280	0
100	90	00	0	-0.01	-0.02	-0.01	-0.02	0.19	0.34	7.13	280	0
100	80	00	0	-0.03	-0.05	-0.02	-0.03	0.73	0.84	7.12	280	0
100	70	00	0	-0.08	-0.11	-0.05	-0.06	1.45	1.48	7.09	280	0
100	60	00	0	-0.16	-0.17	-0.08	-0.06	2.24	2.20	7.05	280	0
100	50	00	0	-0.27	-0.26	-0.11	-0.09	3.10	3.09	6.99	280	0
100	40	00	0	-0.41	-0.38	-0.14	-0.12	3.99	3.87	6.92	280	0
100	30	00	0	-0.57	-0.52	-0.16	-0.14	4.50	4.44	6.84	280	0
100	20	00	0	-0.70	-0.64	-0.13	-0.12	3.81	3.72	6.77	280	0
100	10	00	0	-0.77	-0.71	-0.07	-0.07	2.01	2.03	6.73	280	0
100	00	00	0	-0.80	-0.75	-0.03	-0.04	0.60	0.67	6.72	280	0
100	100	00	5	--	--	--	--	--	--	5.33	284.4	40
100	90	00	5	-0.02	-0.02	-0.02	-0.02	0.52	0.56	5.32	284.4	40
100	80	00	5	-0.07	-0.06	-0.05	-0.04	1.50	1.47	5.30	284.4	40
100	70	00	5	-0.15	-0.13	-0.08	-0.07	2.32	2.28	5.26	284.4	40
100	60	00	5	-0.26	-0.24	-0.11	-0.11	2.91	2.91	5.20	284.4	40
100	50	00	5	-0.38	-0.36	-0.12	-0.12	3.43	3.40	5.14	284.4	40
100	40	00	5	-0.52	-0.49	-0.14	-0.13	3.93	3.85	5.07	284.4	40
100	30	00	5	-0.67	-0.64	-0.15	-0.15	4.26	4.24	5.00	284.4	40
100	20	00	5	-0.81	-0.75	-0.14	-0.11	3.98	3.96	4.93	284.4	40
100	10	00	5	-0.90	-0.84	-0.09	-0.09	2.69	2.69	4.88	284.4	40

100	00	00	5	-0.94	-0.87	-0.04	-0.03	1.03	1.01	4.86	284.4	40
100	100	00	50	--	--	--	--	--	--	4.25	288.3	75
100	90	00	50	-0.02	-0.01	-0.02	-0.01	0.68	0.63	4.24	288.3	75
100	80	00	50	-0.09	-0.04	-0.07	-0.03	1.85	1.76	4.21	288.3	75
100	70	00	50	-0.19	-0.12	-0.10	-0.08	2.71	2.53	4.16	288.3	75
100	60	00	50	-0.30	-0.21	-0.11	-0.09	3.20	3.07	4.10	288.3	75
100	50	00	50	-0.42	-0.32	-0.12	-0.11	3.52	3.50	4.04	288.3	75
100	40	00	50	-0.56	-0.47	-0.14	-0.15	3.81	3.81	3.97	288.3	75
100	30	00	50	-0.70	-0.61	-0.14	-0.14	4.01	4.01	3.90	288.3	75
100	20	00	50	-0.84	-0.73	-0.14	-0.12	3.89	3.82	3.83	288.3	75
100	10	00	50	-0.94	-0.83	-0.10	-0.10	2.95	2.90	3.77	288.3	75
100	00	00	50	-0.99	-0.89	-0.05	-0.06	1.29	1.29	3.75	288.3	75
100	00	00	0	--	--	--	--	--	--	6.72	280	0
90	00	00	0	-0.01	-0.02	-0.01	-0.02	0.33	0.35	6.71	280	0
80	00	00	0	-0.05	-0.06	-0.04	-0.04	1.15	1.12	6.69	280	0
70	00	00	0	-0.13	-0.14	-0.08	-0.08	2.11	2.16	6.65	280	0
60	00	00	0	-0.24	-0.25	-0.11	-0.11	3.17	3.14	6.59	280	0
50	00	00	0	-0.40	-0.40	-0.16	-0.15	4.51	4.54	6.51	280	0
40	00	00	0	-0.62	-0.62	-0.22	-0.22	6.32	6.32	6.39	280	0
30	00	00	0	-0.92	-0.92	-0.30	-0.32	8.35	8.34	6.24	280	0
20	00	00	0	-1.22	-1.22	-0.30	-0.30	8.69	8.62	6.08	280	0
10	00	00	0	-1.39	-1.39	-0.17	-0.17	4.85	4.85	5.99	280	0
00	00	00	0	-1.43	-1.43	-0.04	-0.04	1.26	1.26	5.97	280	0
100	00	00	5	--	--	--	--	--	--	4.85	284.4	40
90	00	00	5	-0.03	-0.03	-0.03	-0.03	0.78	0.73	4.81	284.4	40
80	00	00	5	-0.10	-0.10	-0.07	-0.07	2.13	2.13	4.76	284.4	40
70	00	00	5	-0.21	-0.21	-0.11	-0.11	3.13	3.11	4.69	284.4	40
60	00	00	5	-0.35	-0.34	-0.14	-0.13	3.90	3.82	4.60	284.4	40

50	00	00	5	-0.52	-0.51	-0.07	-0.07	4.79	4.63	4.50	284.4	40
40	00	00	5	-0.73	-0.72	-0.21	-0.21	5.96	5.94	4.37	284.4	40
30	00	00	5	-0.99	-0.97	-0.26	-0.25	7.29	7.23	4.23	284.4	40
20	00	00	5	-1.27	-1.22	-0.28	-0.25	7.83	7.83	4.13	284.4	40
10	00	00	5	-1.46	-1.41	-0.19	-0.19	5.70	5.70	4.09	284.4	40
00	00	00	5	-1.54	-1.49	-0.08	-0.08	2.06	2.05	4.86	284.4	40
100	90	30	5	2.53	2.53	--	--	--	--	5.34	284.4	40
100	80	20	5	2.38	2.38	-0.15	-0.16	4.04	4.02	5.27	284.4	40
100	70	10	5	2.24	2.25	-0.14	-0.13	3.76	3.72	5.20	284.4	40
100	60	00	5	2.12	2.13	-0.12	-0.12	3.43	3.40	5.14	284.4	40
100	50	00	5	1.98	2.01	-0.14	-0.12	3.93	3.85	5.07	284.4	40
100	40	00	5	1.81	1.84	-0.17	-0.17	4.74	4.74	4.99	284.4	40
90	30	00	5	1.60	1.63	-0.19	-0.21	5.76	5.73	4.89	284.4	40
80	20	00	5	1.38	1.41	-0.22	-0.22	6.03	6.03	4.78	284.4	40
70	10	00	5	1.21	1.26	-0.17	-0.16	0.00	0.00	5.65	284.4	40
100	90	30	50	1.19	1.19	--	--	--	--	4.35	288.3	75
100	80	20	50	1.03	1.03	-0.16	-0.16	4.61	4.57	4.27	288.3	75
100	70	10	50	0.85	0.85	-0.18	-0.18	5.01	5.02	4.18	288.3	75

5. Conclusion